Molecular dynamics simulation of a polysorbate 80 micelle in water

Amir Amani[1,2], Peter York[1], Hans de Waard[3] and Jamshed Anwar[1]*

[1]Computational Biophysics Laboratory, Institute of Pharmaceutical Innovation, University of Bradford, BD7 1DP, UK

[2]Department of Medical Nanotechnology, School of Advanced Medical Technologies, Tehran University of Medical Sciences, Tehran, 1417614411, Iran

[3]Department of Pharmaceutical Technology and Biopharmacy, University of Groningen, Antonius Deusinglaan 1,9713 AV Groningen, the Netherland

AUTHOR EMAIL ADDRESS: j.anwar@bradford.ac.uk

RECEIVED DATE (to be automatically inserted after your manuscript is accepted if required according to the journal that you are submitting your paper to)

ABSTRACT

The structure and dynamics of a single molecule of the nonionic surfactant polysorbate 80 (POE (20) sorbitan monooleate; Tween 80®) as well as a micelle of polysorbate 80 in water have been investigated by molecular dynamics simulation. In its free state in water the polysorbate 80 molecule samples almost its entire conformational space. The micelle structure is compact and exhibits a prolate ellipsoid shape, with the surface being dominated by the polar terminal groups of the POE chains. The radius of gyration of the micelle was 26.2 Å. The physical radius, determined from both the radius of gyration and atomic density, was about 35 Å**.** The estimated diffusion constants for the free molecule (1.8×10^{-6} cm^2/s) and the micelle (1.8×10^{-7} cm^2/s) were found to be remarkably close to the respective experimental values. The lateral diffusion of the molecules on the micelle surface was estimated to be 1.7×10^{-7} cm^2/s, which confirms the highly dynamic nature of the micelle structure.

1. INTRODUCTION

Surfactant molecules have an amphiphilic character and structurally consist of at least two moieties, a hydrophilic and a hydrophobic component. In water they can exhibit a rich phase behavior which may include micelles, rod-like structures, bilayers and cubic phases depending on concentration. Just above the limiting monomer solubility (the critical micelle concentration, CMC), surfactant molecules begin to aggregate into micellar structures that are characterized by an inner core comprising the non-polar moieties and an outer interface of polar moieties in contact with the aqueous environment. The driving force for micelle formation is in general terms understood[1-5], the key components being the hydrophobic effect, which excludes the non-polar moieties from the water to the interior of the micelle structure, and an interfacial free energy penalty for the water-micelle interface. These define an energy barrier akin to nucleation that must be surmounted before a micellar cluster can form a stable micelle. There is also a restraint on the maximum size of the stable micelle, which arises from the loss in configurational entropy that results from microphase separation. These constraints yield a free energy surface that has a maximum (the barrier that must be surmounted) followed by a minimum as a function of cluster size, which explains the observed distribution in micelle size, centered around an average size. The average micelle size is characterized by an aggregation number n, the average number of surfactant molecules in a single micelle.

Micelle formation has been investigated extensively using a variety of experimental techniques including nuclear magnetic resonance, electron paramagnetic resonance, light scattering and small angle neutron diffraction[6-7]. This effort has been complemented by

molecular simulation which yields molecular level resolution, dynamics, and in principle certain thermodynamic quantities. The surfactant models employed in such simulations vary from the physics-type models where only the essential features are retained[8-9] to fully atomistic models based on realistic potentials. Notable simulation studies involving realistic models include micelles of ionic surfactants in an aqueous environment e.g. sodium octanoate[10-11] and sodium dodecyl sulfate[12-13], reverse micelles involving sodium di-2-ethylsulfoccinate (AOT)[14], and simulations of micelle self-assembly of dodecylphosphocholine[15], and sodium dodecyl sulfate[16] and of reverse micelles of fluorinated polyether in supercritical CO_2[17]. Of a particular merit are the recent calculations of free energies of micelle formation from molecular simulation[18-19].

Polysorbate 80 (POE (20) sorbitan monooleate, Tween 80; see Figure 1 for structure) is a nonionic surfactant with excellent emulsifying and wetting properties. It is an odourless and tasteless material, generally regarded as nontoxic and non-irritant, and hence is widely used as an emulsifier, solubiliser and a wetting agent in food, cosmetics, and in pharmaceutical applications that include drug delivery systems for oral, parenteral and topical delivery[20]. It is also commonly used in biochemical applications for solubilising proteins and cell cultures.

The polysorbate 80 molecule is a multi-headed structure, with four extended hydrophilic moieties, one of which has a tagged alkyl chain. It is not obvious, unlike linear surfactants, as to what conformation this molecule adopts either as a monomer or within a micelle structure in an aqueous environment, how the molecules pack into a micelle, nor the nature of the surfactant-water interface. Knowledge of the micelle structure of this class of surfactant structures is of fundamental interest being required,

for instance, for successful applications of molecular-thermodynamic theories,[21-22] and is important for technological applications to enable development and control of formulations on a rational basis.

Here, we present molecular dynamics simulations of a single polysorbate 80 molecule and the self assembly of sixty polysorbate 80 molecules in an aqueous environment, with a focus on structural and dynamic properties. Molecular simulation of polysorbate 80 micelles presents somewhat of a challenge as the structure of the molecule is relatively large (214 atoms) with a micelle aggregation number of probably around 60 molecules (the published aggregation number varies widely extending over the range 22–350 [23–27]) . These definitions suggest a molecular system size with explicit water molecules of ~ 100,000 atoms, which whilst doable can challenge laboratory computing facilities. In view of this we have opted for a coarse grained approach wherein a number of atomic sites are represented by a single particle, which makes this system accessible in terms of length and a timescale albeit compromising some atomic detail. These simulations extend the breadth of micelle simulations with respect to the complexity of the surfactant structure investigated.

2. METHODOLOGY

2.1. Molecular structure of polysorbate 80

The chemical structure of the polysorbate 80 molecule is not entirely defined. Polysorbate 80, along with other polysorbates (e.g. polysorbate 20, 40, 60), is defined as being composed of fatty acid esters of sorbitol-derived cyclic ethers having approximately 20 mols of ethylene oxide per mol of polysorbate 80. However, the

distribution of the size of the ethylene oxide groups is not constant and varies from batch to batch[20]. A few attempts have been made to determine the dominant structure for the various polysorbates using a variety of analytical methods[28-31]. For polysorbate 60 the dominant structure was determined as having chains composed of an almost equal distribution of ethylene oxide groups[31]. There is no similar study for polysorbate 80, in view of which we took the lead from the polysorbate 60 study and considered ethylene oxide moieties of equal lengths for the polysorbate 80 molecule (see Figure 1).

2.2. Molecular model

The coarse-grained model for the polysorbate 80 molecule was based on the MARTINI forcefield[32], which is typically based on a "four to one" representation, whereby four heavy atoms of the original molecule plus any associated hydrogen atoms are represented by a single coarse-grained (CG) particle. Where necessary, three to one and two to one representations are also employed[33]. In this study, it became apparent to us that it was possible to map the molecular structure using a three-to-one mapping such that each of the CG particles would be neutral and not be characterized by a partial charge. This removes the need for costly electrostatics calculations within the molecular dynamics simulations, making the simulations considerably more efficient. Thus, each of the three groups $–CH_n–O–CH_n–$, $–CH_n–CH_n–CH_n–$, and $–CH_n–CH_n=CH_n–$ group, where n= 1, 2 or 3 (terminal methyl), were represented by a single CG particle, namely COC, C3 and C32 respectively from the MARTINI forcefield. The $CH_2–O–C=O$ group and $CH_2–O–H$ groups were also taken as individual particles being represented by COCO and COH CG particles respectively from the MARTINI forcefield (see Figure 2). For consistency, we

also used a three to one mapping for the CG representation of water rather than the commonly employed four to one representation.

The masses of the respective CG particles were taken as the sum of the masses of the atoms represented by the given particle (Table 1). The CG particles are connected to each other by harmonic bonds characterized by the potential function $U(r) = 0.5k(r-r_0)^2$. The bond parameters were set as prescribed by MARTINI: the equilibrium distance r_0=4.3Å; the force constant k=12.5 $kJmol^{-1}Å^{-2}$, with the exception of the ring particle for which all connecting bonds had the force constant k=50 $kJmol^{-1}Å^{-2}$. The angles were described by the function $U(\theta) = 0.5k (\cos \theta - \cos \theta_0)^2$ and the equilibrium angles and associated force constants are presented in Table 2. No torsion parameters were considered. The interaction potential for the MARTINI CG particles is of the Lennard Jones (LJ) form $U_{LJ}(r) = 4\varepsilon [(\sigma/r)^{12} - (\sigma/r)^6]$ with no electrostatic interaction. The LJ interaction parameters for the CG particles are given in Table 3.

The molecular dynamics simulations were carried out using DLPOLY_2.19[34] in the NPT ensemble. The temperature and pressure were fixed at 298°K and 1bar, respectively using Berendsen's algorithm with both the thermostat and barostat relaxation times set to 1.0 ps. The cutoff value for van der Waals interactions was 12.0 Å. The timestep employed was 30fs.

The single surfactant molecule simulation was carried out in a simulation box containing 3000 CG water molecules. The self assembly simulation involved 60 surfactant molecules, which is within the experimentally determined range for the aggregation number for polysorbate 80,[23–27] in 10000 CG water particles. This corresponded to a concentration of ~0.1M (CMC= 0.012mM). All molecules were

randomly placed into the simulation box, avoiding strong repulsive contacts. As suggested by the MARTINI forcefield, the overall time was scaled by a factor of 3 to yield the true simulation time which is reported in this paper. The averages and associated uncertainties were calculated using the block averaging technique to minimize correlation errors. The single polysorbate 80 molecule in water was simulated for 20.0 ns of which the first 10 ns was considered as equilibration and the remaining 10 ns for extracting averages. The simulation time after scaling the time axis for the self assembly system was 110 ns, of which the first 10 ns corresponded to equilibration, during which the self assembly of the micelle aggregate took place. The potential energy and the various structural parameters such as radius of gyration and eccentricity all converged rapidly, well within the identified 10ns equilibration period. The remaining trajectory was used for extracting the data averages.

3. RESULTS AND DISCUSSION

3.1 Single polysorbate 80 molecule in water

A series of snapshots of the surfactant molecule from the single molecule simulation trajectory after equilibration are presented in Figure 3. The average values for the lengths of POE chains and the alkyl chain (defined as the distance between the particles numbered 14 and 18, 22 and 26, 27 and 31, and 12 and 8 for the POE chains, and particles 1 and 7 for the alkyl chain) and the radius of gyration are given in Table 4. It appears that the molecule samples its entire conformational degrees of freedom and no single conformation predominates. The individual POE chains spend some of their time in an open structure and the remainder coiled up in a globular form. This behavior is

expected as the $–CH_2–O–CH_2–$ groups and the terminal $–CH_2–OH$ have a strong interaction with water and thus tend not to be trapped in a tight structure. The average length of the POE chains and the alkyl chain is lower than their fully extended length, 14.63 vs 17.2 Å for POE chains and 18.60 vs. 25.8 Å for the alkyl chain, thus revealing on average a degree of compaction for both the hydrophobic and hydrophilic chains. Furthermore, it appears that the head POEs are able to stretch more freely compared to the tail POE, the POE chain connected directly to the alkyl chain.

The packing parameter P for a molecule is defined by

$$P = \frac{V}{a_0 l_c}$$

where V is the volume of the hydrophobic tail, a_o is the headgroup area, and l_c is the maximum length of the tail[35]. The packing parameter is useful in predicting the geometrical properties of aggregates of surfactants[36]. Thus, spherical, cylindrical, vesicular, planar bilayers, or inverted micelle structures are characterized by packing parameter values of $P < 1/3$, $1/3 < P < 1/2$, $1/2 < P < 1$, $P \sim 1$ and $P > 1$, respectively. For the isolated polysorbate 80 molecule the volume of the hydrophobic tail was given by $V=(27.4 + 26.9n)$ Å^3 for n carbon atoms, and $l_c = (1.5 + 1.265n)$ Å. The headgroup area a_o was calculated by projection of the headgroup along the vector between the head group and the tail onto the perpendicular plane. The packing parameter was estimated to be 0.07, predicting a spherical shape for the formed micelles, as one might expect from the gross features of the polysorbate 80 molecules notably a very large headgroup and a relatively short tail.

To look at the hydration of the molecule more closely, the various CG particles in the polysorbate 80 molecule were split into three separate groups, namely, hydrophobic (i.e. C32 and C3), hydrophilic (ie. COC and COCO) and terminal polar (i.e. COH). The radial pair distribution function, g(r), for each of these against water (shown in Figure 4) exhibits a shell of hydration. The average number of the water particles within the hydration shell (up to the first minimum in the g(r)) for each of the molecular groups were C3 (19.4), C32 (17.7), COCO (22.7), COC (21.9) and COH (32.1). As Figure 4 and the hydration numbers suggest, the hydration around the hydrophobic and hydrophilic parts of polysorbate 80 show the expected rank order but is on whole pretty much similar, other than the number of water particles around the terminal polar groups being considerably greater as would be expected. The hydration shell around the core of the molecule is limited relative to other groups possibly because of the limited accessibility of this region due to the four moieties branching from the core structure. Clearly the coarse graining removes the sharp distinction in hydration of a hydrophilic and a hydrophobic moiety that might be observed at an atomic resolution.

3.2 Micelle self assembly

Snapshots of the micelle self-assembly process are shown in Figure 5. The randomly positioned molecules of polysorbate 80 first aggregate into small clusters, which then come together to form a single micelle, the entire process taking about 800ps. All 60 molecules become integrated into the micelle. The micelle then undergoes restructuring to yield its final equilibrium arrangement. The resulting micelle shows stability over the full residual trajectory with no indication of breaking up and no tendency for the

individual molecules to leave the micelle structure over the simulation period. The variation in potential energy of the system during and after the assembly process is given in Figure 6. It shows a sharp fall over the first ~800ps, reflecting the assembly of the monomers, and then only a gradual decrease that corresponds to the restructuring of the micelle.

3.3. Micelle structure

We first focus on the shape and size of the micelle. Figure 7 shows a snapshot of the micelle along with a cross-sectional view from the trajectory. The micelle is compact exposing the terminal polar particle at the surface while the alkly chains, as expected, occupy the central core. The variation in the radius of gyration (R_g) as a function of simulation time is presented in Figure 8, whilst the average radius of gyration (R_g) and the shape parameters of the micelle are tabulated in Tables 4 and 5, respectively. The radius of gyration R_g shows little variation after equilibration, the average value being 26.2Å. There is no available experimental value to compare against. The physical radius of the micelle can estimated from the gyration radius using $R_m = \sqrt{\frac{5}{3}} R_g$,[37] which yields a radius of 33.8 Å. Whilst we have taken the aggregate number of 60 polysorbate 80 molecules for the simulations (the basis being the study of de Campo et al.[26]) the experimental literature reveals considerable inconsistency, making comparison with experiment difficult. The published aggregation number varies widely extending over the range 22−350 whilst the associated micelle radius ranges 2.1−4.05 nm respectively[23−27].

In characterizing the shape of the micelle we assumed it be ellipsoidal characterized by the three semiaxes, a, b, and c which were calculated from the principal axes of inertia of the micelle $I_1 > I_2 > I_3$ using

$$I_1 = \frac{1}{5} M (a^2 + b^2)$$
$$I_2 = \frac{1}{5} M (a^2 + c^2)$$
$$I_3 = \frac{1}{5} M (b^2 + c^2)$$

where M is the total mass of the micelle.

The eccentricity was calculated using

$$e = \sqrt{1 - \frac{c^2}{a^2}}$$

The ratio of the average semi-axes is 1.25 : 1.12 : 1.00 indicating that on average the shape of the micelle is prolate ellipsoid i.e. like that of a rugby ball. Such a shape has been reported for micelles of a number of other surfactants (eg.[14,38]). The eccentricity (after equilibration) as a function of time varies over the range 0.45–0.75 (Figure 9) indicating minor fluctuations in shape.

The average atomic-density profiles computed with respect to the centre of mass of the micelle are given in Figure 10. The effect of the micelle deviating from a spherical shape was ignored; the implication is that the calculated density distributions may be broader than they actually are. The molecular structure of the polysorbate 80 was divided into four distinct groups: the hydrophobic tail consisting of particles numbered 1-6 (i.e. C3 and C32), the ring or core part of the molecule comprising particles 19, 20 and 21, the

terminal polar particles (COH) numbered 18, 26 and 31, and the hydrophilic part comprising the remaining molecule (i.e. COC and COCO particles).

We note that the water density begins to decrease from the bulk value of ~970 kg/m^3 (which is similar to the experimental value) as we move into the micelle. Water molecules are able to penetrate the micelle up to about 18 Å from the centre of the micelle whilst the hydrophobic moieties of the polysorbate 80 molecule can extend outwards to about 26 Å from the centre. Thus we have an inner hydrophobic core of about 22 Å with a buffer zone of about ± 4 Å. Whilst the water molecules, the ring structure, and the terminal polar groups of the POE chains are restricted to being outside the hydrophobic core, there appears to be considerable overlap between the hydrophilic POE chains and the alkyl chains, covering a region from about 12 to 26 Å. The density of the hydrophobic core is about 800 kg/m^3 which is slightly higher than the experimental density value of 785 kg/m^3 for pure 1-heptadecene[39], suggesting well packed liquid-like structure. The outer layer of the micelle is dominated by the terminal polar groups of the POE chains due to strong interactions between these particles and the water. Analysing the total density reveals a peak region where the density is higher than that of the bulk water and the micelle interior and is thought to arise from the high density central ring structure of the molecule. The density distribution also enables the estimation of the micelle radius. Taking the peak to peak distance between the opposing polar terminal particles yields a micelle radius of about 35 Å which is close the value of about 34 Å obtained from the radius of gyration. In summary, as expected, the hydrophobic tail occupies the inner core of the micelle while the terminal polar groups of the POE chains form a shell around the micelle, with the ring component being located within the centre

of the headgroup. There does not appear to be any significant void space within the micelle.

We also characterised the surface topology, in particular the extent of openness of the micelle surface by calculating the surface accessible area using a spherical probe with a radius of 4.3 Å i.e. the van der Waals radius of the CG particles. The solvent accessible area was calculated using VMD version 1.86 and was determined to be 15528 $Å^2$. The surface area of a smooth ellipsoid of the same size as the micelle calculated using

$$S = 4\pi\left(\frac{a^p b^p + b^p c^p + a^p c^p}{3}\right)^{1/p}$$

with p=1.6075,[40] is 14212 $Å^2$. The accessible surface area is higher as one might expect but not by that much given the probe molecule is a coarse-grained particle. A visual view of the micelle surface reveals it to be rather compact and non-porous (see Figure 7).

3.4 Structure of the polysorbate 80 molecule *within* the micelle

A particularly important question is what is the average molecular conformation of the molecule in the micelle, the average here being defined as spatial over all molecules in the micelle, and temporal over the entire trajectory after equilibration. To this end distributions of characteristic distances, angles, and a particular torsion were calculated and are presented in Figures 11-13 respectively. The distributions of the vector lengths of the POE chains all essentially superimpose, being relatively sharply peaked at about 15 Å with variation over the range 10-18 Å. This suggests that these chains are rather bent yielding a compact head group. The alkyl chain vector length is characterised by a

slightly broader distribution peaking at about 20 Å, whilst the end-to-end vector length for the combined POE and alkyl chain shows a very broad distribution ranging from 10 to 40 Å. The latter clearly shows that the tail part of the molecule samples a large amount of conformational space within the micelle and that there is no strong preference for it to being straight. Indeed this is confirmed by the distribution of the angle defined by the atoms (18,13,8) which is indicative of how bent are the combined POE and alkyl tails (Figure 12). This angle shows a wide distribution ranging from 50 to 180°, peaking at about 140°. A straight tail would yield an angle of 180°. The angle distributions in Figure 12 also reveal that the tails do not in general point to the centre of the micelle. The angle defined by the vector linking core atom 13 to the terminal alkyl atom 1 (i.e. the combined POE and alkyl tail) and the vector from atom 13 to the centre of mass of the micelle shows a rather sharp peak at about 25°, suggesting a significant misalignment from the micelle centre. An angle of zero would mean that the tails point towards the micelle centre. The polysorbate 80 structure has a number of torsions around the core ring structure that define the rotation of the POE chains relative to each other, an important one being the torsion angle between either of the POE chains defined by atoms 21−26 or 20−31 and the POE chains defined by atoms 13−18 or 13−8. The distributions of these torsions were calculated and that defined by atoms (28,20,13,15) is given in Figure 13. These distributions suggest some preference for two of the POE chains, atoms 27−31 and 22−26, to form a V-like structure, the centre of which is perpendicular to the other two POE chains (atoms 14−18 and 8−12) that form an almost linear backbone (see Figure 14).

We also determined the averaged conformation of the molecule within the micelle, averaging over all molecules within the micelle and over the entire trajectory after equilibration. Taking one of the molecules from the first configuration of the trajectory as a basis, the other molecules were superimposed onto this molecule using the rigid-body Kabsch algorithm[41]. This algorithm superimposes either the centres of mass or the coordinates of a selected atom of two molecular structures (conformations) and then calculates the optimal rotation matrix that minimizes the root mean squared deviation (rmsd) between identical atoms in the two molecular conformations. Superpositions based on one of the atoms representing the core ring structure (atom 19), rather than the centre of mass, were found to give lower rmsds and hence are reported here. The remarkable, cactus-like 'average' structure of the polysorbate 80 molecule alongside a composition of all superposed conformations is given in Figure 14. The average structure reveals an almost linear backbone comprising a POE chain linked to the alkyl tail, and two short arms corresponding to the other two POE chains. The three POE chains with polar terminal groups all point away from the centre of the micelle, exposing the polar terminal groups to the solvent. These POE chains along with the alkyl tail are considerable shortened, with the CG particles showing extensive overlap that in energetic terms would be, were it to be a real effect, wholly unfavorable. This shortening and the particle overlaps are essentially artifacts of the averaging. The actual molecules sample all kinds of conformations where the chains are either slightly bent or coiled but because these conformations are distributed evenly (by definition) about the mean coordinates, the mean coordinates reflect a projection of the actual coordinates. Hence, it becomes clear

that the average structure as determined is not a real conformation in which the molecule spends its predominant time.

The 'composition' of the superposed conformations of the polysorbate 80 molecules within the micelle in Figure 14 provides an alternative perspective. This clearly reveals that the molecules sample their conformational space as well as the local physical volume within the micelle rather uniformly. Again it may be tempting to suggest that this is the textbook pinhead representation of the polysorbate 80 molecule. This would be misleading. The composite structure could represent the physical volume sampled by a single polysorbate 80 molecule and this in itself would be true. However, it *does not* represent the excluded volume between two interacting molecules within a micelle. Within the micelle, there is much accommodation and cooperation between the molecules to yield a compact structure.

The packing parameter of the surfactant molecules was also computed after equilibration based on the equations given in Section 3.1. The headgroup area for the polysorbate molecule in the micelle was estimated from the separation distance between respective core (the central ring) regions of the molecules. The packing parameter of the polysorbate 80 in the micelle was estimated to be 0.12, which as expected is a little larger than the value of 0.07 calculated for the free molecule in water, reflecting the constraints on the headgroups from neighbouring molecules within the micelle.

3.5 Dynamics

The diffusion constants for the free molecule and the micelle were calculated from the mean squared displacement of the centre of mass of the molecule or micelle using the

Einstein relationship $d = \langle \Delta r^2 \rangle / 6t$, where $\langle \Delta r^2 \rangle$ is the average mean squared displacement over the time period *t.* The lateral diffusion of the polysorbate molecule on the spherical surface of the micelle was calculated by removing contributions of the centre of mass displacement as well as the rotation of the micelle and projecting the resulting displacement of the individual molecules onto the spherical surface, i.e. onto the perpendicular plane defined by the outward vector from the centre of the micelle. Lateral diffusion being 2-dimensional was calculated using the relationship $d = \langle \Delta r^2 \rangle / 4t$. The diffusion constant for the free molecule in water was estimated to be 1.8 x 10^{-6} cm^2/s, which is remarkably close to the corresponding experimental value of 1.9 x 10^{-6} cm^2/s obtained using pulsed field gradient spin echo NMR[42]. The calculated diffusion constant for the micelle was 1.8 x10^{-7} cm^2/s which compares well with the experimental estimate of 3.0 x10^{-7} cm^2/s[42], making the self-diffusion of the free molecule about 10-fold faster. The lateral means squared displacement of the individual molecules on the spherical surface of the micelle revealed diffusional behavior rather than reaching a plateau, confirming that the micelle structure is not lattice-like. The calculated lateral diffusion of the individual surfactant molecules was 1.7 x10^{-7} cm^2/s, that is, about the same as that of the micelle.

4. SUMMARY AND CONCLUSION

The POE sorbitan esters are a rather complex class of surfactants comprising multiple chains that are highly flexible. The structure of these molecules in their free state in water and that of the micelle aggregates that they form has been outstanding for some time. We

have carried out molecular dynamics simulations of polysorbate 80 as a single free molecule as well as the self-assembly of a micelle comprising 60 (the known micelle aggregation number) polysorbate molecules in water, and characterized both structural aspects and dynamics. For efficiency we opted for a coarse grained model representation of the molecule – the polysorbate 80 molecule contains 214 atoms and makes the overall system size rather large. The relatively decent reproduction of the experimental data suggests that the loss of specificity is not an issue; indeed this was expected as there are no strong, specific interactions that could be compromised in going to a coarse grained representation. In its free state in water, the polysorbate molecule samples its almost entire conformational space, with the alkyl tail at times being completely exposed to the water environment. As would be expected, its estimated packing parameter (0.07) in the free molecule state suggests a very large effective headgroup and a relatively short tail. The simulations reveal that the self-assembly of a micelle of polysorbate 80 from randomly dispersed molecules is extremely fast, occurring within a nanosecond of simulation time. The resulting micelle is stable for the entire trajectory lasting 110 ns. The micelle structure is compact with the surface being dominated by the polar terminal groupds of the POE chains, and exhibits a prolate ellipsoid shape that shows minor fluctuations. The average radius of gyration was 26.2 Å whilst the physical radius was about 35 **Å.** The hydrophobic core of the micelle is densely packed with a density slightly higher than that of a medium chain liquid alkane. Within the micelle, the 'average' structure of the polysorbate 80 is best described as cactus-like with the polar terminal groups of 3 of the POE chains all bidding to be at the water interface. The molecule, while constrained within the micelle structure, is anything but rigid and samples almost

its entire conformational space. The estimated diffusion constants for the free molecule (1.8×10^{-6} cm^2/s) and the micelle (1.8×10^{-7} cm^2/s) were found to be remarkably close to the respective experimental values. The lateral diffusion of the molecules on the micelle surface was about the same as that of the micelle structure. These structural and dynamical insights set the foundation for exploring the next stage of complexity concerning these surfactants, namely emulsification and in particular nanoemulsions[43,44] that serve as drug delivery carriers for pharmaceutically-active hydrophobic molecules that are challenging to deliver by other means.

ACKNOWLEDGMENT

The study has been supported by Tehran University of Medical Sciences & Health Services grant number 88-01-87-8624.

REFERENCES

1. L. Maibaum, A. R. Dinner, D. Chandler, *J. Phys. Chem. B,* 2004, *108*, 6778.

2. R. Nagarajan, E. Ruckenstein, *Langmuir,* 1991, *7*, 2934.

3. B. C. Stephenson, K. Beers, D. Blankschtein, *Langmuir,* 2006, *22*, 1500.

4. C. Tanford, *J. Phys. Chem,* 1974, *78*, 2469.

5. C. Tanford, *Proceedings of the National Academy of Sciences of the United States of America,* 1974, *71*, 1811.

6. M. C. Jones, J. C. Leroux, *Eur. J. Pharm. Biopharm,* 1999, *48*, 101.

7 C. C. Müller-Goymann, *Eur. J. Pharm. Biopharm,* 2004, *58*, 343.

8. K. Esselink, P. A. J. Hilbers, N. M. Van Os, B. Smit, S. Karaborni, *Colloids Surf. A. Physicochem. Eng. Asp,* 1994, *91*, 155.

9. B. J. Palmer, J. Liu, *Langmuir,* 1996, *12*, 6015.

10. J. C. Shelley, M. Sprik, M. L. Klein, *Langmuir,* 1993, *9*, 916.

11. K. Watanabe, M. Ferrario, M. L. Klein, *J. Phys. Chem,* 1988, *92*, 819.

12. C. D. Bruce, M. L. Berkowitz, L. Perera, M. D. E. Forbess, *Phys. Chem. B,* 2002, *106*, 3788.

13. A. D. MacKerell Jr, *J. Phys. Chem,* 1995, *99*, 1846.

14. S. Abel, F. Sterpone, S. Bandyopadhyay, M. Marchi, *J. Phys. Chem. B,* 2004, *108*, 19458.

15. S.J. Marrink, D. P. Tieleman, A. E. Mark, *J. Phys. Chem. B,* 2000, *104*, 12165.

16. M. Sammalkorpi, M. Karttunen, M. Haataja, *J. Phys. Chem. B,* 2007, *111*, 11722.

17. L. Lu, M. L. Berkowitz, *J. Am. Chem. Soc,* 2004, *126*, 10254.

18. R. Pool, P. G. Bolhuis, *J. Phys. Chem. B,* 2005, *109*, 6650.

19. B. C. Stephenson, K. A. Stafford, K. J. Beers, D. Blankschtein, *J. Phys. Chem. B* 2008, *112*, 1641.

20. R. C. Rowe, P. J. Sheskey, A. J. Owen, *Handbook of pharmaceutical excipients*; London UK and American Pharmaceutical Association: Washington, 2005.

21. B. C. Stephenson, A. Goldsipe, K. J. Beers, D. Blankschtein, D. *J. Phys. Chem. B,* 2007, *111*, 1025.

22. B. C. Stephenson, K. Beers, D. Blankschtein, *Langmuir,* 2006, *22*, 1500.

23. Md. E. Haque, A. R. Das, S. P. Moulik, *Journal of Colloid and Interface Science* 1999, *217*, 1–7.

24. R. K. Mahajan, J. Chawla, M. S. Bakshi, G. Kaur, V. K. Aswal, P. S. Goyal, *Colloid Polym. Sci.* 2004, *283*, 164–168.

25. L. de Campo, A. Yaghmur, N. Garti, M. E. Leser, B. Folmer, O. Glatter, *Journal of Colloid and Interface Science* 2004, *274*, 251–267.

26. K. M. Glenn, S. Moroze, R. M. Palepu, S. C. Bhattacharya, *Journal of Dispersion Science and Technology*, 2005, *26*, 79–86.

27. A. Amani, Ph.D. Thesis, University of Bradford, 2008.

28. F. O. Ayorinde, S. V. Gelain, J. H. Johnson Jr, L. W. Wan, *Rapid Commun. Mass. Spectrom,* 2000, *14*, 2116.

29. J. D. Brandner, *Drug Dev. Ind. Pharm,* 1998, *24*, 1049.

30. S. Frison-Norrie, P. Sporns, *J. Agric. Food Chem,* 2001, *49*, 3335.

31. V. Dang, *J. Pharm. Biomed. Anal,* 2006, *40*, 1155.

32. L. Monticelli, S. K. Kandasamy, X. Periole, R. G. Larson, D. P. Tieleman, S. J. Marrink, *J. Chem. Theory. Comput,* 2008, *4*, 819.

33. S. J. Marrink, H. J. Risselada, S. Yefimov, D. P. Tieleman, A. H. de Vries, *J. Phys. Chem. B,* 2007, *111*, 7812.

34. W. Smith, T.R. Forester, *J. Molm Graph,* 1996, *14*, 136.

35. C. Tanford, *J. Phys. Chem,* 1972, *76*, 3020.

36. J. N. Israelachvili, S. Marelja, R.G. Horn, *Q. Rev. Biophys,* 1980, *13*, 121.

37. S. H. Chen, *Ann Rev Phys Chem*, 1986, *37*, 351.

38. S. Senapati, J. S. Keiper, J. M. DeSimone, G. D. Wignall, Y. B. Melnichenko, H. Frielinghaus, M. L. Berkowitz, *Langmuir,* 2002, *18*, 7371.

39. D. R. Lide, CRC Handbook of Chemistry and Physics, Taylor & Francis: 2009.

40. R. F. Burton, *Biomedical calculations: principles and practice*; John wiley: Chichester, 2008.

41. W. Kabsch, *Acta Crystallogr,* 1976, *32*, 922.

42. G. Lafitte, K. Thuresson, P. Jarwoll, M. Nyden, *Langmuir,* 2007, *23*, 10933.

43. M. J. Lawrence, G. D. Rees, *Adv. Drug. Deliv. Rev,* 2000, *45*, 89.

44. D. K. Sarker, *Current Drug Delivery* 2005, 2, 297-310.

FIGURES

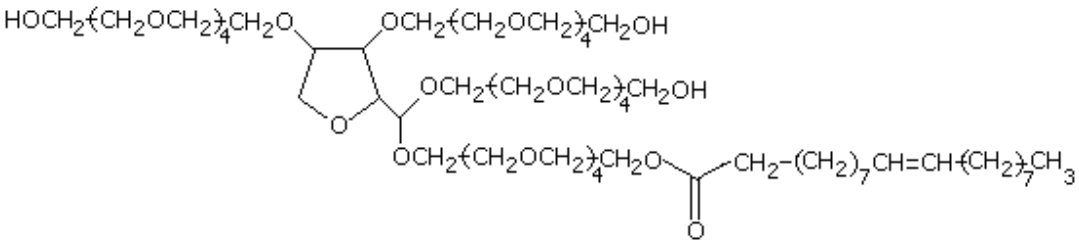

Figure 1. Molecular structure of polysorbate 80.

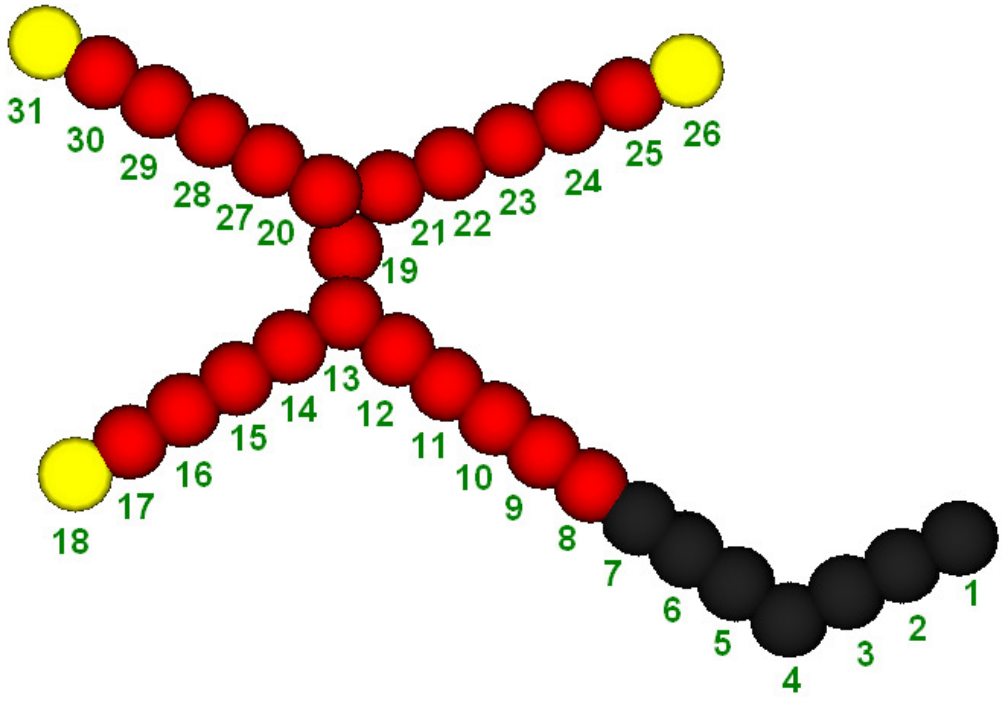

Figure 2. Coarse grained model of polysorbate 80 molecule. Hydrophilic (ie. COC and COCO), hydrophobic (ie. C3 and C32), and terminal polar groups (ie. COH) of the polysorbate 80 are represented as red, black and yellow particles, respectively.

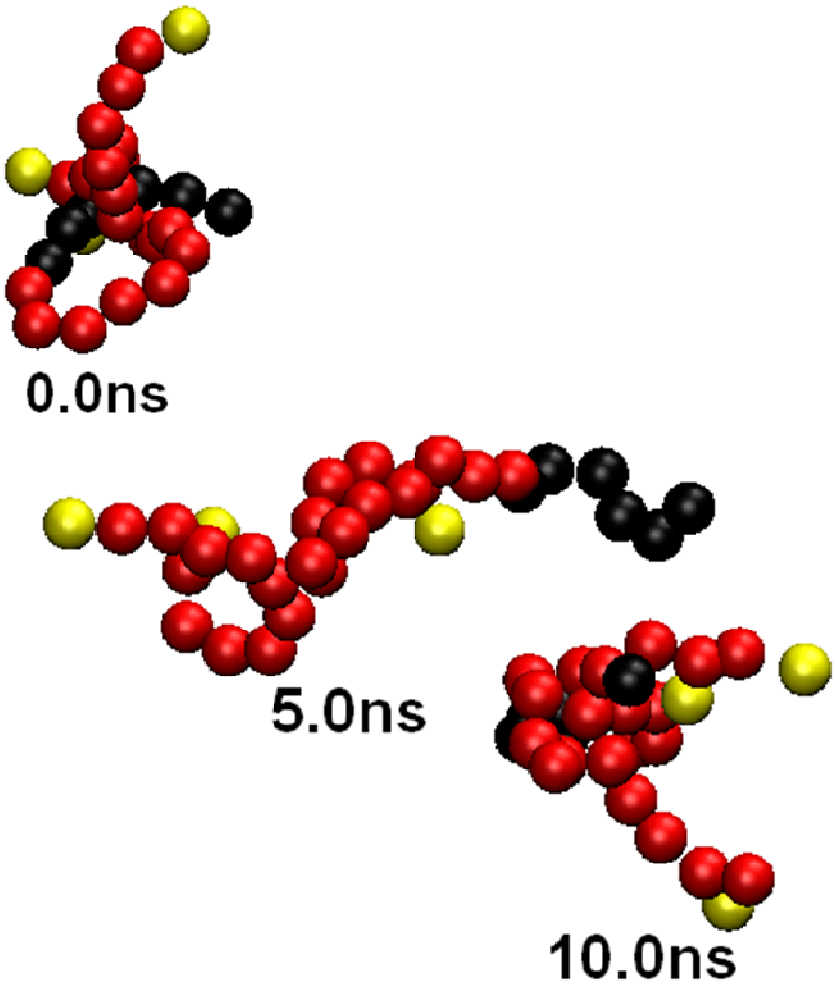

Figure 3. Snapshots from a trajectory of a single molecule of polysorbate 80 in water. Red particles represent the hydrophillic moieties (i.e. COC and COCO particles), black particles characterize the hydrophobic moieties (i.e. C3 and C32 particles), and yellow particles represent the terminal polar groups (i.e. COH).

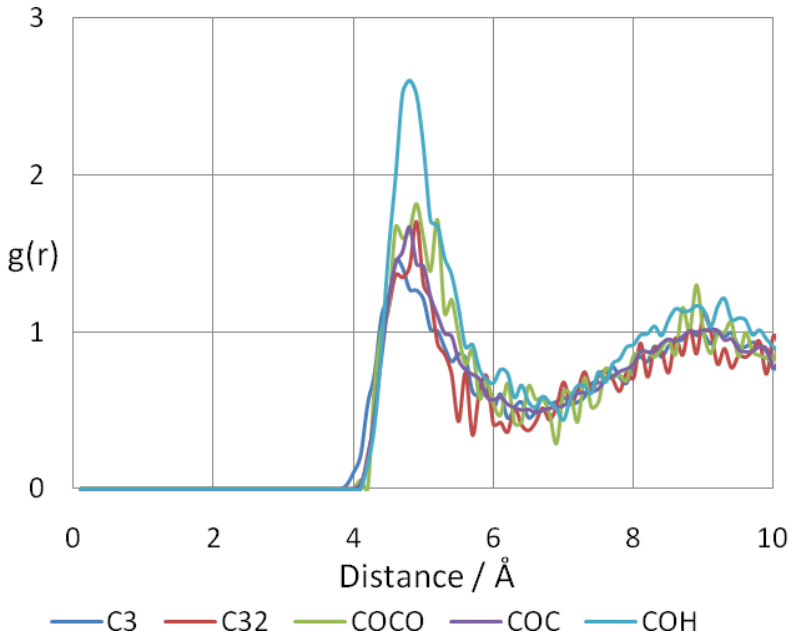

Figure 4. Averaged radial pair distribution functions for the various coarse-grained particle types with water particles for the single polysorbate 80 molecule in water.

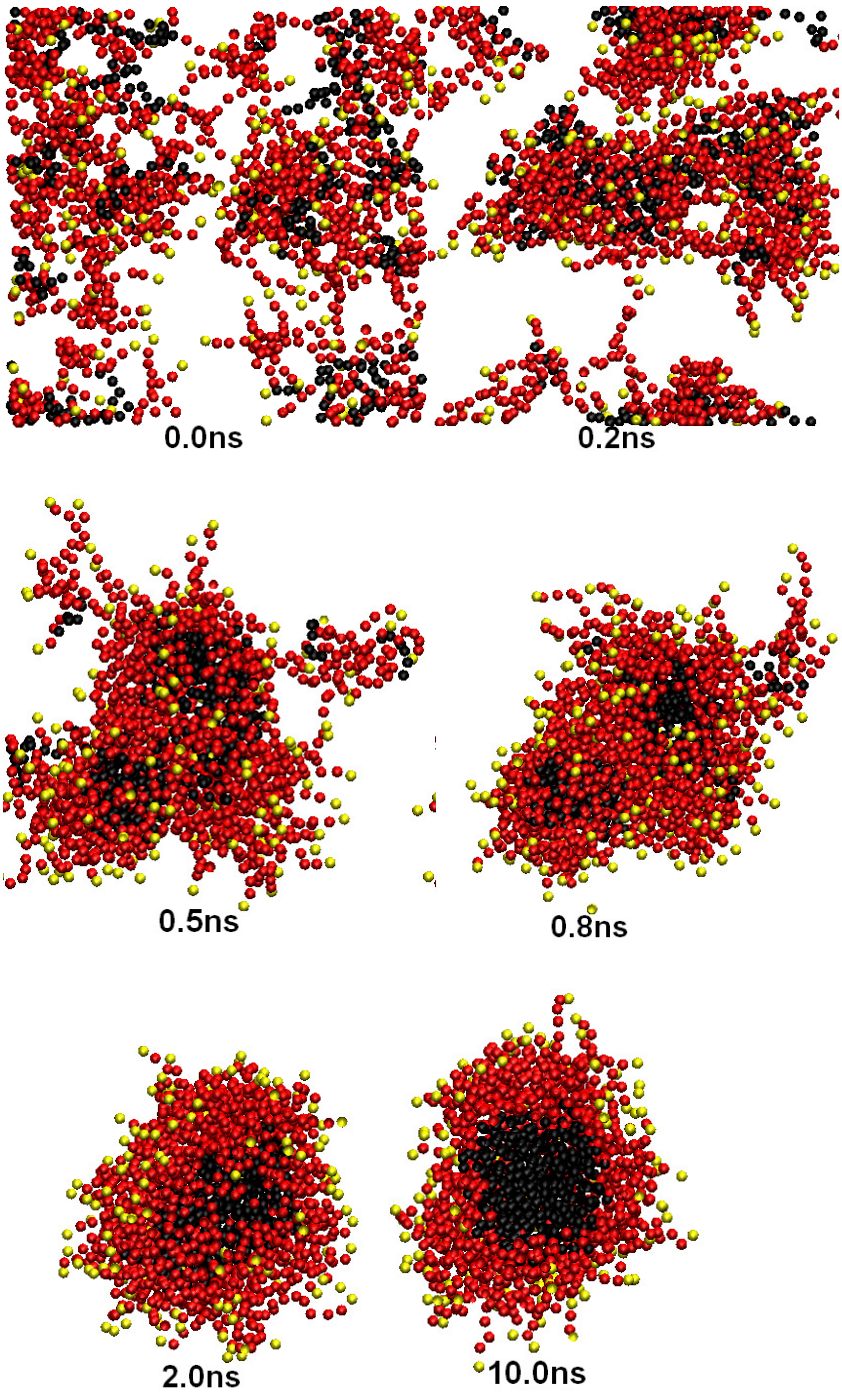

Figure 5. Snapshots of the self assembly of polysorbate 80 molecules to yield a micelle.

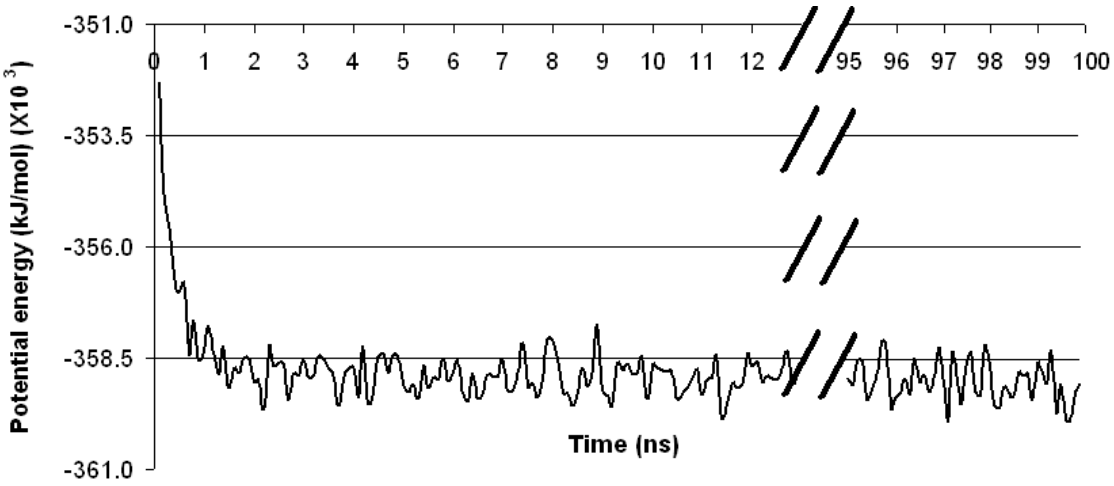

Figure 6. Variation of the potential energy of the system during and after self-assembly of the micelle.

.

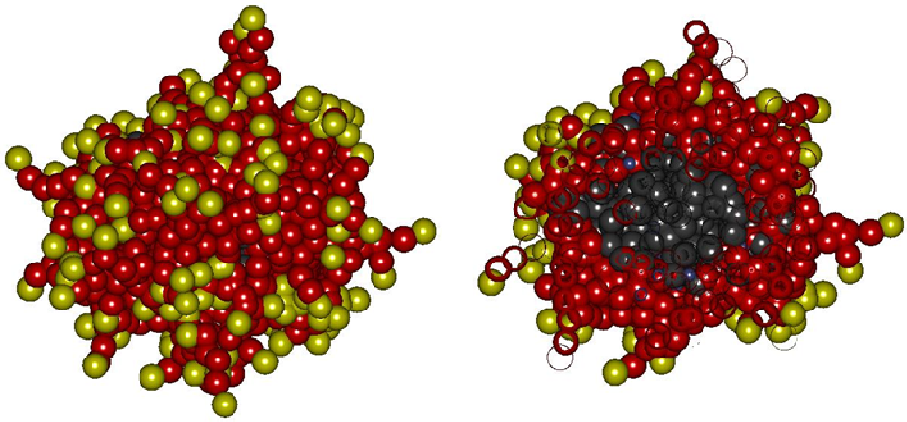

Figure 7. Snapshot of the polysorbate 80 micelle along with a cross-sectional view 37.5 ns into the simulation trajectory.

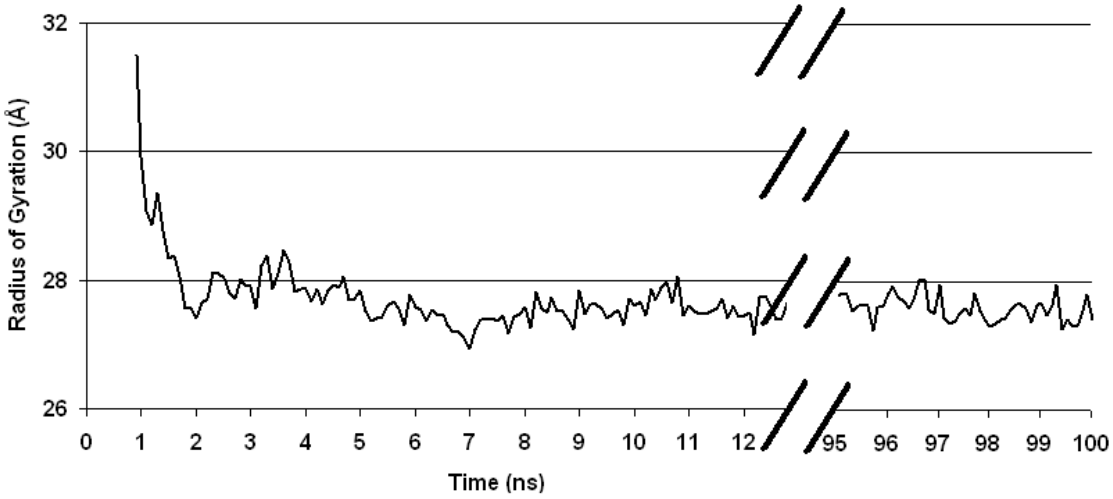

Figure 8. Radius of gyration (averaged over all molecules) for the polysorbate 80 micelle as a function of simulation time.

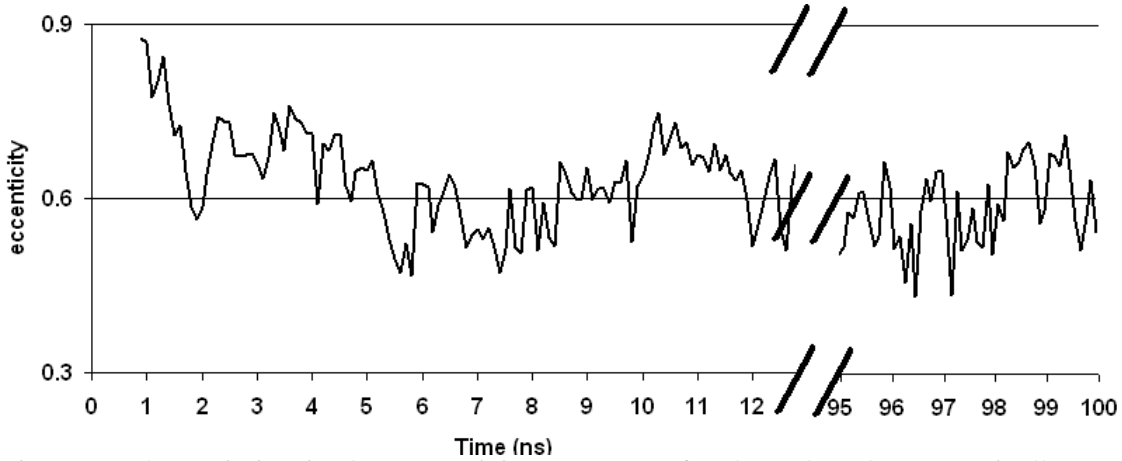

Figure 9. The variation in the eccentricity parameter for the polysorbate 80 micelle as a function of time during and after equilibration.

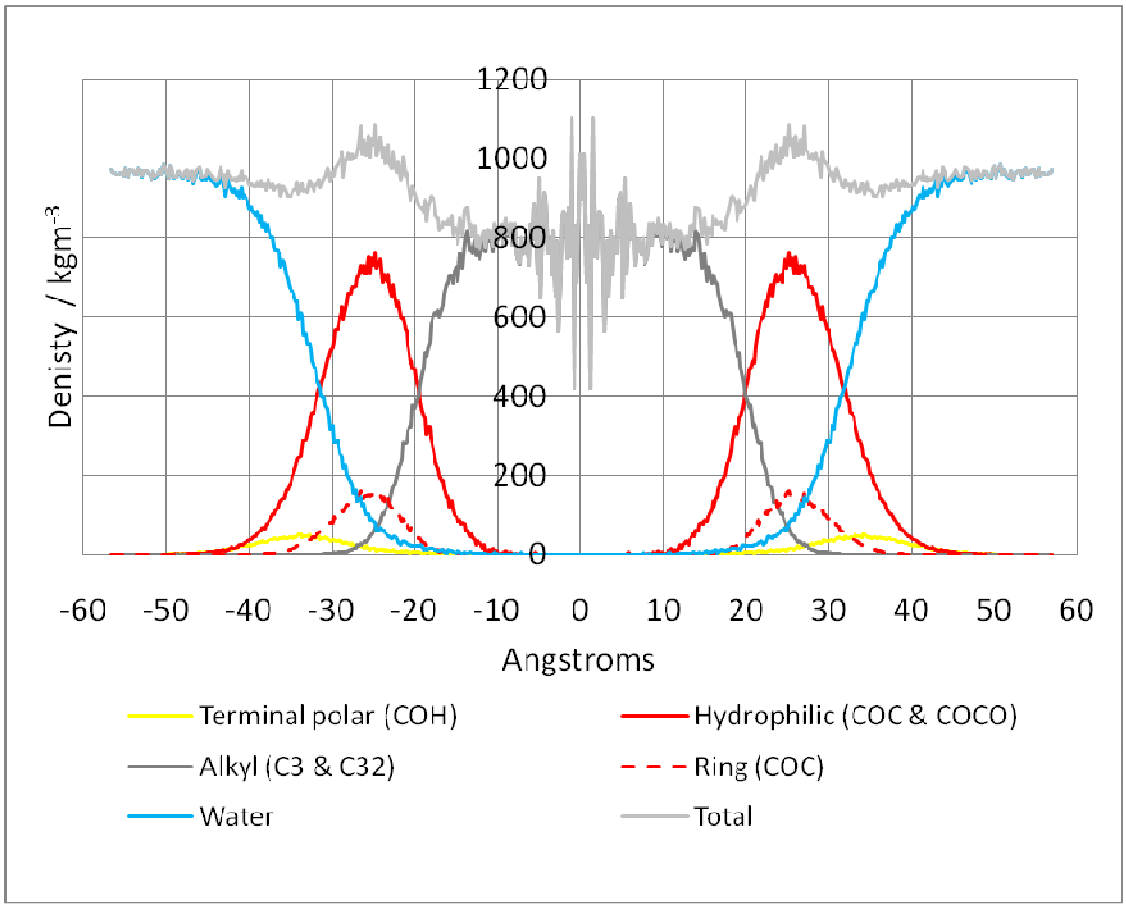

Figure 10. Density distribution of polysorbate 80 moieties from the micelle centre of mass.

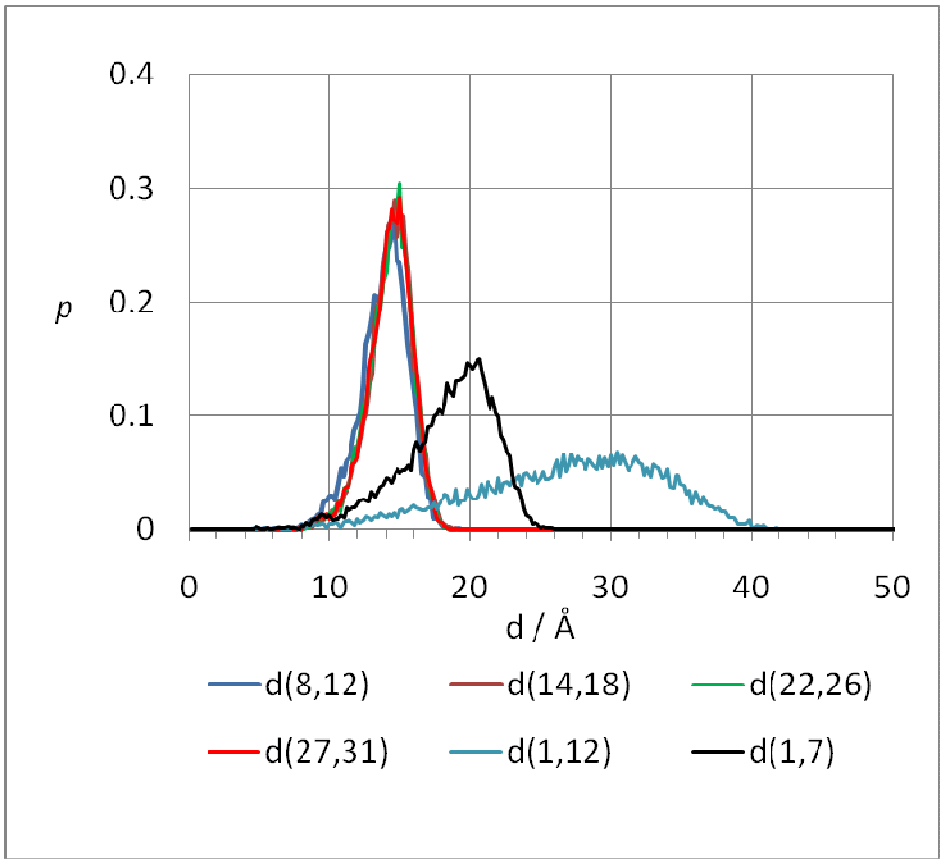

Figure 11. Distributions for characteristic intra-molecular (atom indices given) distances in polysorbate 80 molecules comprising the micelle.

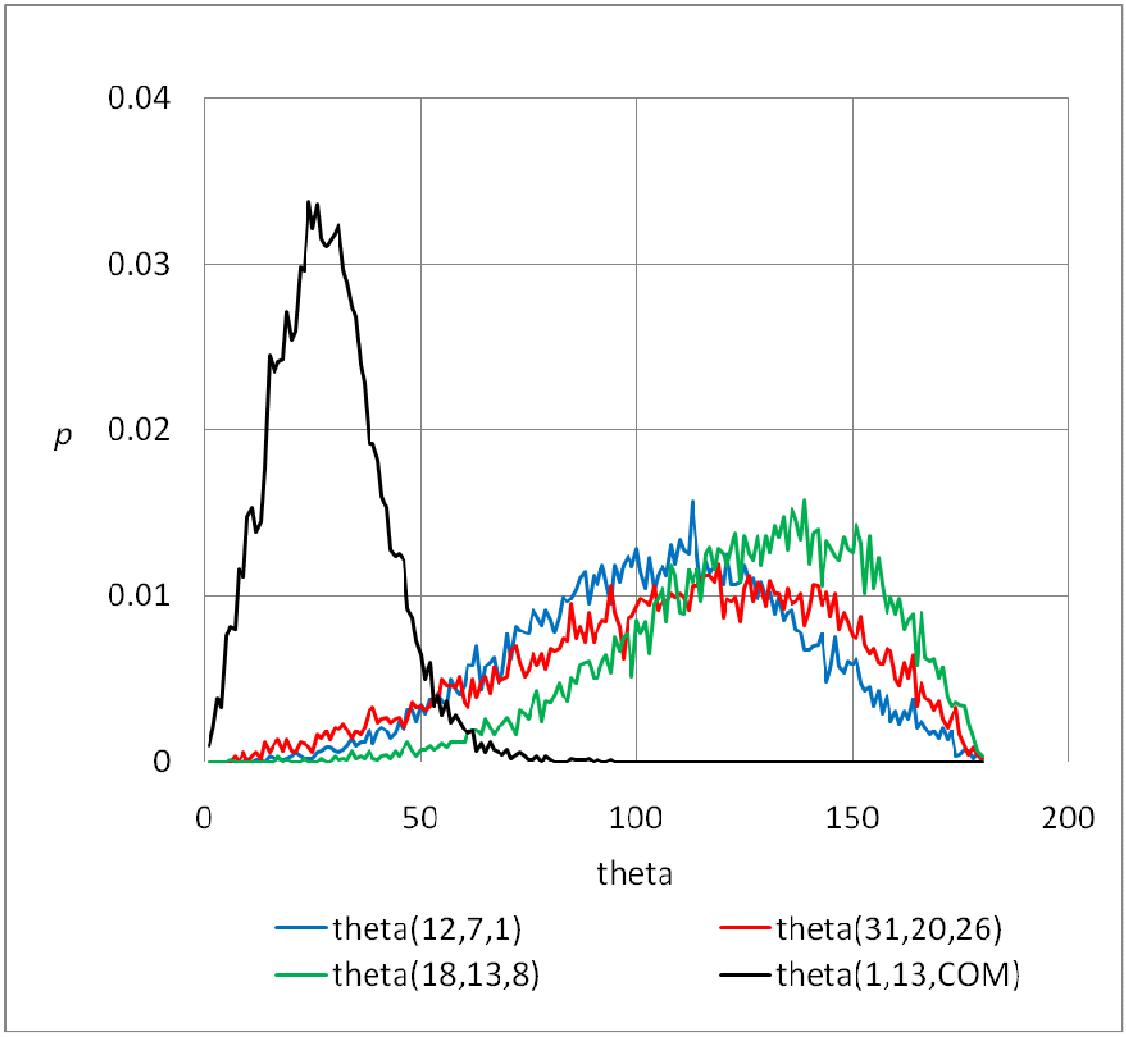

Figure 12. Distributions for characteristic intra-molecular (atom indices given) angles in polysorbate 80 molecules comprising the micelle.

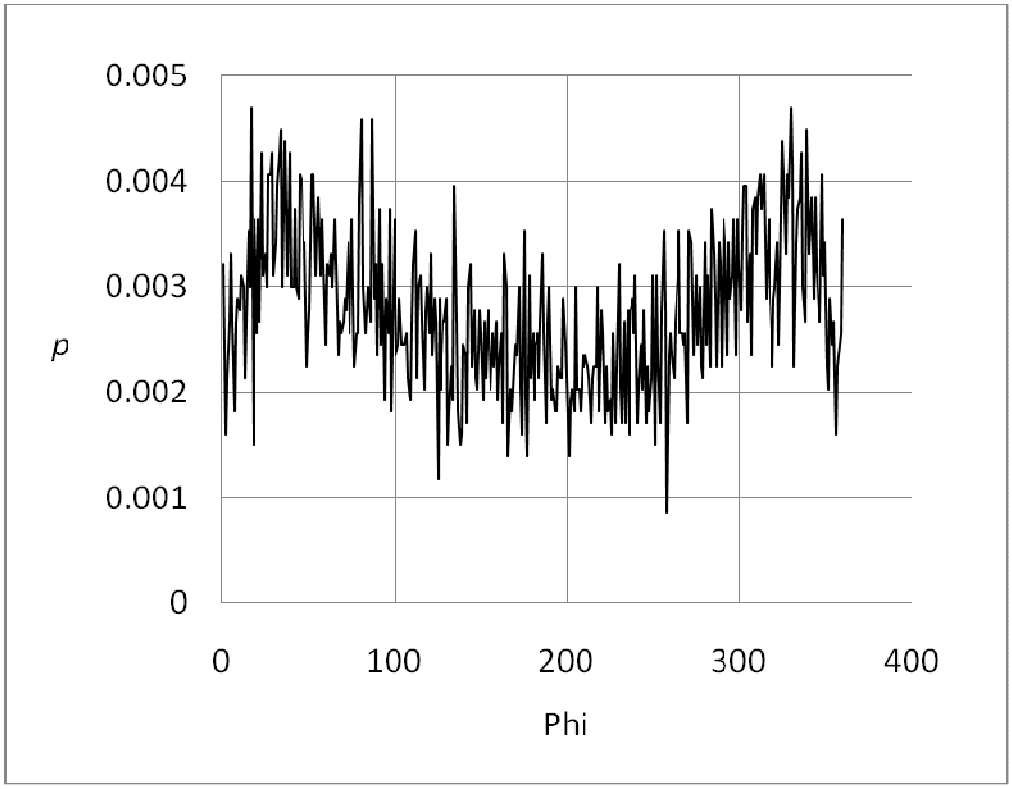

Figure 13. Distribution for the torsion angle defined by ϕ (28,20,13,15), where the integers represent atom indices. This torsion defines the rotation of one of the two linked POE chains with terminal polar groups relative to the POE-alkyl tail backbone of the molecule (see Figure 14).

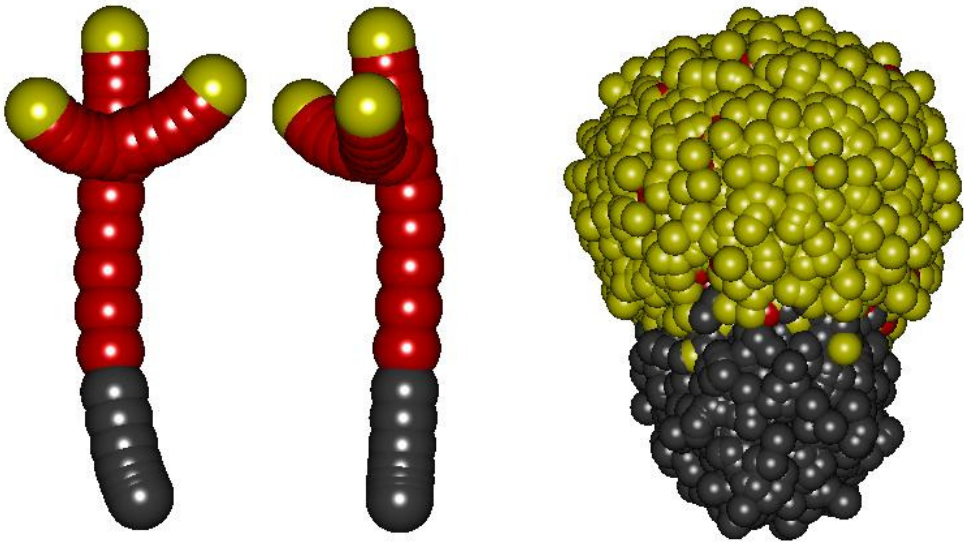

Figure 14. Left: ‘Average’ structure of polysorbate 80 molecule in the micelle determined by superimposing all molecules within the micelle over the entire trajectory after equilibration. Right: Composition of the superposed polysorbate 80 molecules.

Table 1. Masses assigned to coarse-grained particles of polysorbate 80

Particle type	Mass / amu
COH	31
COC	44
C3	40
C32	38
COCO	58

Table 2. Angle bending parameters for polysorbate 80 molecule

Angle definition		Beads number	Force constant k / kJmol^{-1}	Ideal angle θ_0 / degrees
C3-C32-C3			45	120
COC-COC-COC	chain-ring-ring	12-13-19 13-19-20 22-20-21	25	120
COC-COC-COC	ring-ring-ring	20-21-19 21-20-19 20-19-21	25	120
all others			25	180

Table 3. Lennard Jones interaction parameters for polysorbate 80.

Particle Interaction	ε	δ
C3 – C3	3.2	4.3
C3 – COCO	2.5	4.3
C3 – COC	2.5	4.3
C3 – COH	2.1	4.3
C3 – W	1.8	4.3
C32 – C3	3.2	4.3
C32 – COCO	2.5	4.3
C32 – COC	3.2	4.3
C32 – COH	2.3	4.3
C32 – W	2.0	4.3
COCO – COCO	3.0	4.3
COCO – COC	2.6	4.3
COCO – COH	3.4	4.3
COCO – W	3.4	4.3
COC – COC	2.6	4.3
COC – COH	2.6	4.3
COC – W	3.0	4.3
COH – COH	3.8	4.3
COH – W	3.4	4.3
W – W	3.4	4.3

Table 4. Average lengths and associated standard deviations for the various moieties and the hydrophobic alkyl chain, and the radius of gyration averaged over the trajectory for the isolated (single molecule simulation) molecule of polysorbate 80 in water and for the micelle comprising sixty polysorbate 80 molecules.

	Radius of gyration (Å)	Average length of head-POE chain (Å)	Average length of tail-POE chain (Å)	Average length of alkyl chain (Å)
Isolated molecule	10.61 (1.91)	14.63 (0.99)	12.40 (2.09)	18.7 (5.35)
.Micelle	27.55 (0.20)	14.96 (1.08)	13.77 (1.97)	21.96 (3.81)
Micelle core	15.77 (0.31)	–	-	–

Table 5. Semiaxes of the micellar ellipsoid where a, b and are ellipsoid semiaxes and e is eccentricity.

	a (Å)	b (Å)	c (Å)	<a/c>	e
Micelle	37.42	33.62	29.93	1.25	0.60
Core	23.12	20.15	17.30	1.34	0.66